J Mol Model (2009) 15:223–232
DOI 10.1007/s00894-008-0397-6

ORIGINAL PAPER

Theoretical study on the ground state intramolecular proton transfer (IPT) and solvation effect in two Schiff bases formed by 2-aminopyridine with 2-hydroxy-1- naphthaldehyde and 2-hydroxy salicylaldehyde

N. Tezer · N. Karakus

Received: 19 July 2008 / Accepted: 3 October 2008 / Published online: 2 December 2008

Abstract The tautomerization mechanism the isolated and monohydrated forms of two Schiff bases 1 and 2, and the effect of solvation on the proton transfer from enol-imine form to the keto-enamine form have been investigated using the B3LYP hybrid density functional method at the 6-31G** basis set level. The barrier heights for H_2O-assisted reactions are significantly lower than that of unassisted tautomerization reaction in the gas phase. Nonspecific solvent effects have also been taken into account by using the continuum model (IPCM) of four different solvent. The tautomerization energies and the potential energy barriers are decreased by increasing solvent polarity.

Keywords Density functional theory · Enol-imine · Keto-enamine tautomerizm · Schiff bases · Solvent effect

Introduction

Proton tautomerism is a general phenomenon in organic molecules and has a vital role in many fields of chemistry and biochemistry. The study of ground state intramolecular proton (hydrogen) transfer (IPT) reactions have received increasing attention in recent years aiming at the characterization of a large number of compounds in which rapid hydrogen migration occurs both in solution and in solid state. Reversible solid state thermal reactions are of interest due to their potential usage as a basis for optical data storage devices [1–3].

Salicilidine aniline and its derivatives are among the earliest examples of a chemical system involving IPT. A prototropic tautomeric attitude has been recognized in a number of aromatic Schiff bases [4–11]. 2-Hydroxy schiff base ligands are of interest mainly due to the existence of OH....N and NH....O type hydrogen bonds and tautomerism between the enol imine and keto-enamine forms. 2-Hydroxy schiff base ligands and their complexes derived from the reaction of salicylaldehyde and 2-hydroxy-1-naphthaldehyde with amines have been extensively studied [12–17] and a group of them were common as models for biological systems [18–22]. Tautomerism in 2-hydroxy Schiff bases both in solution and in solid state were investigated using different spectroscopic techniques [23–40] and theoretical methods [41, 42]. In the spectra of solutions of these compounds, different Schiff bases have been studied in both polar and non-polar solvents [23–25, 27, 43–46]. In the solid state, salicylidine anilines take part mostly in the enol-imine tautomeric form. In naphthaldimines both forms are possible and OH....N and NH....O intramolecular hydrogen bonds may occur [29, 39, 47–49]. The keto-enamine tautomer is always observed when the Schiff base is derived from 2-hydroxy naphthaldehyde and aniline, on the other hand the keto-enamine form was not observed in polar and non-polar solvents but was noted after acid addition [4, 34, 50, 51].

In the present work, we have studied IPT of the Schiff bases formed by 2-aminopyridine with 2-hydroxy-1- naphthaldehyde and 2-hydroxy salicylaldehyde (Scheme 1, **1** and **2**) in order to compare the hydrogen bonding and tautomerism in these compounds. Particular attention is given to solvent effects and to the comparison of the available experimental

N. Tezer (✉) · N. Karakus
Faculty of Arts and Science, Chemistry Department,
Cumhuriyet University,
58140 Sivas, Turkey
e-mail: ntezer@cumhuriyet.edu.tr

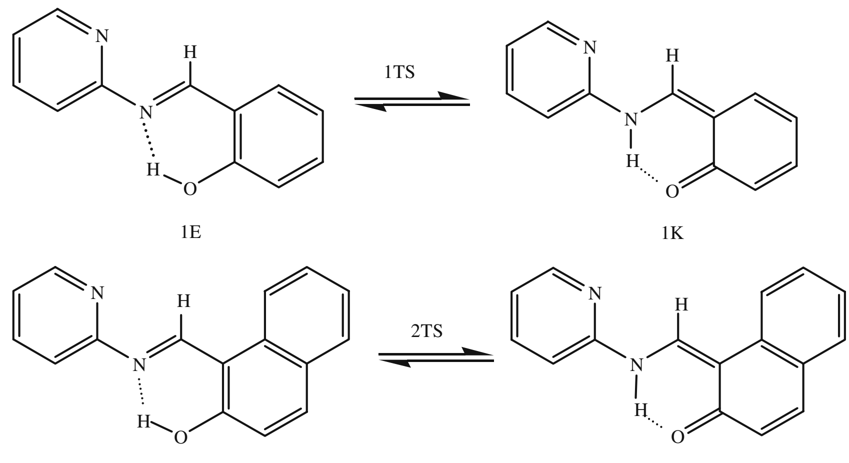

Scheme 1 Intramolecular proton transfer process of studied Schiff bases

data. The full discussion and comparison between two molecules will be the subject of the forthcoming letter.

Method

The ground state geometries of the reactants, transition states and products for tautomerization of the isolated and monohydrated complexes are optimized by using the most popular B3LYP [52–54] method applying the 6-31G** basis sets without any symmetry restrictions in the gas phase. The vibrational frequencies have been obtained at the same level for the characterization of the local minimum and the transition states (corresponding to a single negative eigenvalue of the Hessian). The Nonspecific solvent effects of the solvent medium were studied by means of the IPCM [55] model. The IPCM model has been used for energy calculations with a different dielectric constants (ε=4.9, $CHCl_3$; ε=24.55, C_2H_5OH; ε=46.7, DMSO; ε=78.54, H_2O). For the specific solvent effects like H-bonds, calculations with the inclusion of one water molecule as solvent to the enol-, keto- forms and TS structures have been carried out. We have performed calculations at the same level of theory for the complexes. Basis set superposition error (BSSE) is calculated using MASSAGE keyword. The electronic structures of the stationary points were analyzed by the natural bond orbital (NBO) [56, 57] method. All calculations were carried out with the Gaussian 03 program package [58].

Results and discussion

Structures

DFT calculations at the B3LYP/6-31G** level have been performed for the tautomeric equilibria of two Schiff bases, N-(2-pyridil)-salicylidene (**1**) and N-(2-pyridil)-2-oxo-1-naphthylidenemethylamine (**2**). The compounds, shown in Scheme 1, exist as enol-imine (**E**) and keto-enamine (**K**) tautomeric forms. First, we started our investigation to find the most convenient conformation of the title compounds in the gas phase. To determine the conformational energy profiles (for the **E** forms), the optimized geometries were kept fixed, and values of the DFT energies were calculated as the functions of the torsion angles $\theta_1(N_2C_5N_1C_6)$ and $\theta_2(C_{12}C_7C_6N_1)$ from 0° to 360°, varied every 30°. The results were illustrated in Fig. 1. The molecular energies were calculated as a function of each torsional angle (θ), keeping the other torsional angles constant. The optimized torsion angles θ_1 and θ_2 of the Schiff bases **1E** and **2E** are 0.00°, −179.99° and −0.05°, 179.98°, respectively. The energy profile as the function of θ_1 shows one maxima near 180° because of the steric interactions between H_2 and H (C_4) atoms. The conformational energy as a function of θ_2 shows a maxima near 90°. The interaction between the N lone pair and π-electrons of the rotated phenyl ring or naphthyl ring might contribute to the conformational energy of enol forms.

Table 1 shows the important geometrical parameters of ach tautomeric and transition state (TS) forms. Compared to the experimental data [59], the calculated geometries at this level had small average errors in bond lengths and in bond angles. The optimized geometrical parameters indicate that two forms of the Schiff bases **1** and **2** are whole planar, which are in agreement with the experimental and semi-empirical values [59, 60]. The planarity of the structures is attributed to (a) the orientation of the pyridine ring: the hetero N-atom is cis with respect to the H_2 and (b) the strong intramolecular H-bond, which locks the salicylaldimine group. In these planar molecules, there is no strain between the hetero N-atom and H_2 (distance $N_2....H_2$ is 2.3–2.4 Å in the keto-enamine and enol-imine forms). The experimental value is 2.5 Å [60].

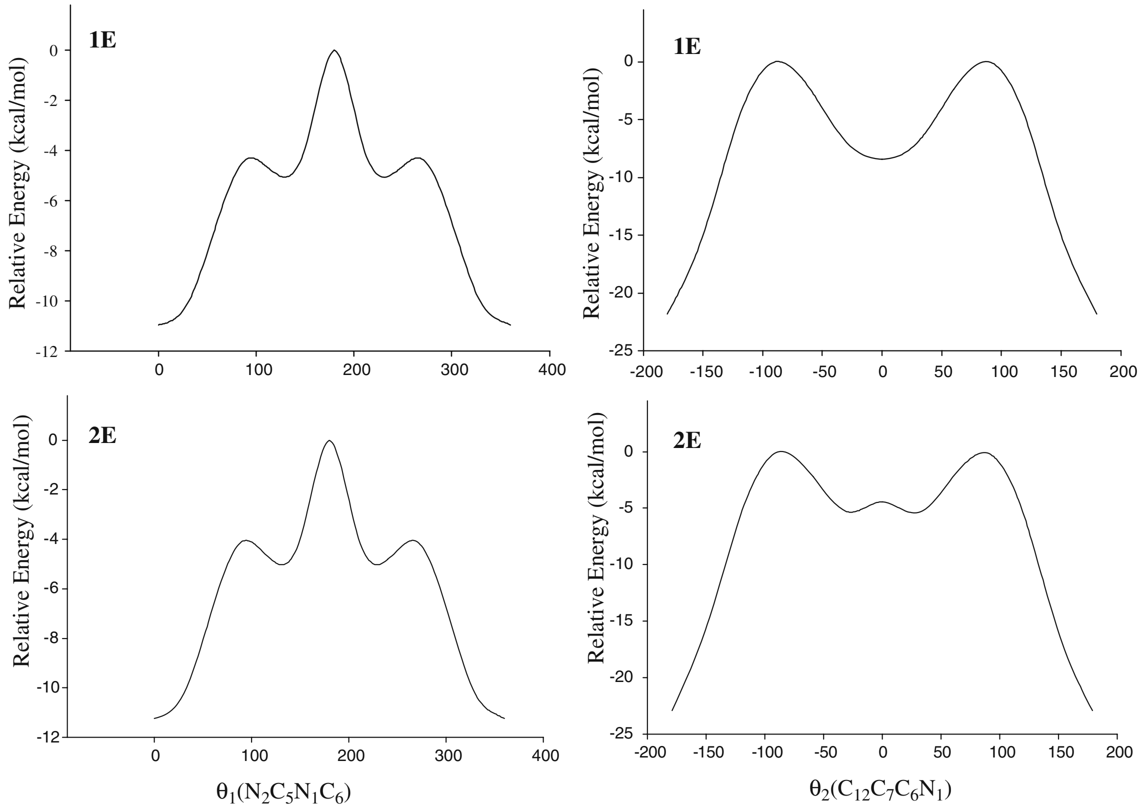

Fig. 1 Calculated conformation energies for optimized structures (**1E** and **2E**) of θ_1 and θ_2 torsion angles

The N-O distance apparently gives a good indication of H-bond strengths, whereas the N-H lengthening due to strong H-bond formation is small or even irrelevant [61]. According to the numerical values of bond lengths and interatomic distances, the intramolecular OH....N hydrogen bond in **2** (1.616 Å) seems to be stronger than the intramolecular hydrogen bond in **1** (1.705 Å). It has a shorter donor- acceptor distance in **2E** (2.541 Å) than those of the hydrogen bond in **1E** (2.611 Å). Also the H....acceptor distances are in line with this conclusion (see Fig. 2).

In the enol-imine forms, the C_8-O_1 bond lengths 1.334–1.330 Å are smaller than the single bond in phenol's (1.343 Å) and greater than the double bond in ketones (1.210 Å) [62–65]. In the structure of the Schiff base ligand **2**, when the enol-imine form is transformed into the keto-enamine form, an appreciable increase in the C=N distance (about 0.04 Å) and a concomitant decrease in the C-O distance (about 0.07 Å) is observed. The shortening in the C-O bond length can be explained by the quinoiodal structure (keto-enamine form) as in the 2-hydroxy-1-naphthaldimine derivatives [39, 40, 66, 67]. The C_6-N_1 and C_8-O_1 bond lengths are consistent with similar compounds [68–71].

The proton transfer reaction E → K has been considered. For the enol-imine forms of the two compounds, the bond lengths (C_8-O_1, C_8-C_7, C_7-C_6, C_6-N_1) are between single bond length and double bond length, which indicates that a conjugative system is composed of O_1, C_8, C_7, C_6, N_1 and H_1. The conjugative effect also exists in the compound keto-enamine forms. The transfer of hydrogen atom from N_1 to O_1 atom is accompanied by a rearrangement of the whole six-membered ring, and substantial changes are observed in the carbon-oxygen and carbon-nitrogen bonds.

The transition states, shown in Fig. 2, are found to be planar. Their geometries are listed in Table 1. The transition states for intramolecular proton transfer was calculated, and the first saddle point existence was confirmed. The distance between oxygen and hydrogen (O_1-H_1) enlarges, while the one between nitrogen and hydrogen (N_1-H_1) reduces on the proton transfer 1E → 1TS → 1K and 2E → 2TS → 2K. The N_1-H_1 and O_1-H_1 distance for **1TS** is 1.198 Å and 1.288 Å, respectively. It can be concluded that the O-H bond is broken and N-H bond is formed during the proton transfer process in the Schiff base ligand **1**. Considering **2TS**, the N-H bond is broken and O-H bond is formed (The N_1-H_1 and O_1-H_1 distance is 1.242 Å and 1.227 Å, respectively). In the proton transfer E → TS → K; C_8-O_1 and C_7-C_6 distances decrease, and the C_8-O_7 and C_6-N_1 distances increase, while the angle $<C_7C_8O_1$ decreases first and then increases. The $<C_6N_1H_1$ angle become larger on E → K transfer, while the angle $<C_8O_1H_1$ becomes shorter.

Table 1 Selected optimized geometries for all species in the gas phase

	1E	1TS	1K	2E	2TS	2K
Bond lenghs (Å)						
N_1-H_1	1.705	1.198	1.048	1.616	1.242	1.039
N_1-C_5	1.407	1.399	1.398	1.405	1.398	1.396
N_2-C_5	1.342	1.339	1.336	1.342	1.340	1.337
O_1-H_1	1.000	1.288	1.660	1.014	1.227	1.683
O_1-C_8	1.338	1.293	1.264	1.330 (1.279)	1.296	1.259 (1.263)
O_1-N_1	2.611	2.416	2.564	2.541 (2.518)	2.399	2.559 (2.586)
C_7-C_8	1.426	1.452	1.470	1.416 (1.436)	1.439	1.470 (1.445)
C_7-C_6	1.444	1.413	1.393	1.439 (1.392)	1.414	1.388 (1.380)
C_6-N_1	1.298	1.320	1.337	1.304 (1.317)	1.321	1.343 (1.330)
Bond angles (^{0})						
$<C_8O_1H_1$	106.86	103.46	103.55	106.62	103.99	104.36
$<C_6N_1H_1$	99.84	105.85	111.44	100.65	104.87	112.33
$<C_7O_8O_1$	121.77	120.82	122.08	122.36 (122.70)	121.45	122.73 (122.30)
$<C_7C_6N_1$	121.74	119.15	121.79	121.77	119.84	123.03
$<C_6C_7C_8$	121.27	118.18	119.84	119.26 (118.40)	117.16	118.65 (119.60)
$<O_1H_1N_1$	148.51		141.30	149.34 (136.06)		138.89 (137.09)
$<C_6N_1C_5$				123.20		124.20
$<N_2C_5N_1C_6$	0.00	0.00	0.00	−0.05 (−0.95)	0.00	−0.02 (−3.18)
$<C_5N_1C_6C_7$	−179.99	179.99	179.99	179.98 (179.39)	180.00	180.00 (−178.53)
$<C_7C_8O_1H_1$	0.00	0.01	−0.05	0.00	0.00	0.00
$<C_{12}C_7C_8O_1$	179.99	179.99	−179.97	−179.98 (−179.67)	180.00	−179.99 (177.84)
$<C_6C_7C_8O_1$	0.00	0.00	0.00	0.02 (5.45)	0.00	0.01 (−0.29)
$<C_{12}C_7C_6N_1$	−179.99	−179.99	−179.99	179.98	180.00	−179.99

Available experimental data are also given in parenthesis (taken from [59]). For numbering of the atoms see Fig. 2

Stabilizations and tautomerization energies

The tautomerization energy calculated as a difference in energy between tautomers and transition states in the gas phase and solutions are presented in Fig. 3. For the compound **1**, the enol form is computed to be more stable than the keto form in the gas phase and in solutions. Naphthyl derivative exhibits a different behavior. In the case of compound **2**, the keto form (**2K**) was computed to be more stable than the enol form (**2E**). Previously, the tautomeric behavior of compounds naphthylidene anilines differ considerably from that of corresponding salycylidene anilines [33, 72], which exist mainly in the E-form at room temperature, even in polar solvents. The UV-visible spectra of some 2-hydroxy schiff bases were also studied in polar and non-polar solvents [12, 73]. The keto-enamine tautomer is always observed when the schiff bases are derived from 2-hydroxy naphthaldehyde and aniline. For the schiff bases derived from salicylaldehyde and aniline, the keto-enamine form was not observed in polar and non-polar solvents, but was noted after acid addition. Such a difference could be caused by the loss of aromaticity in going from **E** to **K** form, while in compound **2** this effect is compensated by the transfer of aromaticity within the naphthalene fragment. In the compound **1**, the number of delocalized electrons in the tautomeric phenyl ring is reduced from six to four in going to the K form because two of those electrons are engaged in the strong C=N and C=O bonds. Thus, the phenyl ring loses much of its aromaticity. In the naphthalene compound **2** this effect is compensated by the second aromatic ring. Our gas-phase calculations indicated that 1E → 1K tautomerization reaction has an electronic endothermicity of 3.75 kcal/mol and an activation energy of 5.19 kcal/mol. The comparison of the hydrogen-bond distances of these tautomers reveals the contraction of the O....N distance (Table 1). In contrast for 2E → 2K tautomerization process showed that the reaction has an electronic exothermicity of −0.39 kcal/mol an activation energy of 2.57 kcal/mol. The hydrogen-bond distances of the two tautomers reveals the expand of the O....N distance. The calculations predict the O....N distance to be 2.51 Å in 2E, which is shorter by 0.070 Å than the value calculated for **1E**. In addition, the N....H distance is considerably shorter in **2E** form than the **1E** form. One of these results we predict is the existence of weak intramolecular hydrogen bond in **1E**. The gas phase calculations clarify that compound **1** prefers O-H form and the compound **2** prefers the N-H form.

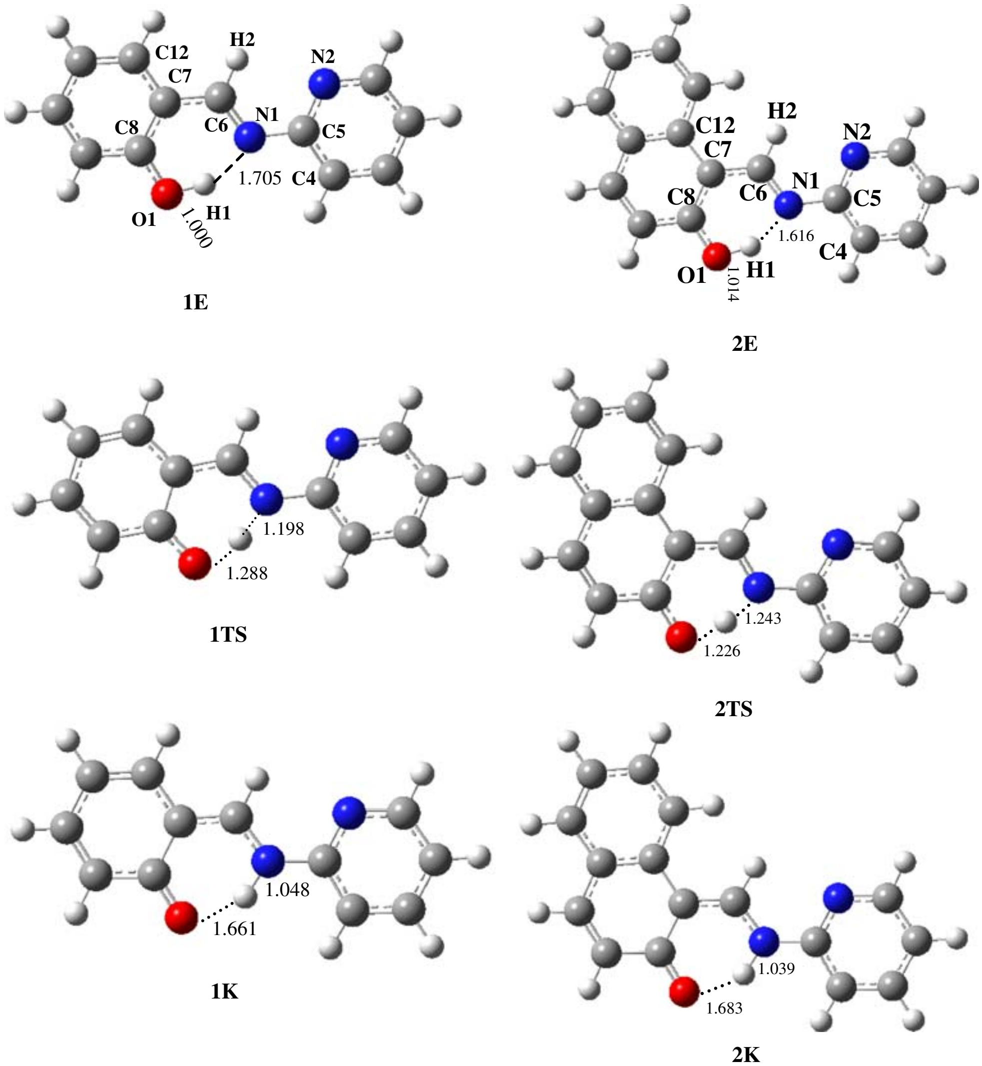

Fig. 2 Optimized tautomer molecular structures of **1** and **2** and transition states (TS) related to the proton transfer process. Atom numbering used in this work is shown

Solvent effects

The standard approach of the IPCM (without any explicit solvent molecules), as it is used here, appears to be a good first step in the theoretical investigation of the effect of solvent on tautomeric equilibrium of Schiff bases **1** and **2**. The energy of each tautomer in the presence of a continuous solvent dielectric was explored to determine the effects of a solvents dielectric on the tautomer energy differences. All the species were stabilized by the dielectric constant of the solvent.

As it can be seen from Fig. 3, the tautomeric equilibrium of **1** is in favor of the enol-imine form, the equilibrium of **2** is in favor of the keto-enamine form both gas phase and solutions. These results agree with the experimental findings of Nazir et al. [59] In their studies ^{1}HNMR data for compound **1** showed that the tautomeric equilibrium favored the enol-imine in $CDCI_3$. The compound **2** shifts to the keto-enamine form in $CDCI_3$.

The energy difference between **1E** and **1K** tautomers decreases on going polar medium. The barrier height of the proton transfer 1E → 1K diminishes considerably from $CHCl_3$ to more polar solvent. The keto-enamine form was also considerably stabilized by the solvation as shown (Figs. 3 and 4). The higher solvation energy (ΔE_s) of the **1K** form results in the lower energy difference between the **1K** and **1E** forms. In addition, the computed dipol moment of **1K** is larger than those of **1E** in different solvents (Table 2). In the process of intramolecular proton transfer, the dipol moments increase notably both 1E → 1K and 2E → 2K, which is agreement with variation trend of the stability and the barrier height of proton transfer reaction. Considering the definition $\mu=\rho.l$, where "ρ" is the charge of the molecule and "l" is the distance between the positive charge center and the negative charge center of the molecule, the variance of charge is very important for the dipole moment. It can be presupposed that the polar solution will facilitate the intramolecular proton transfer

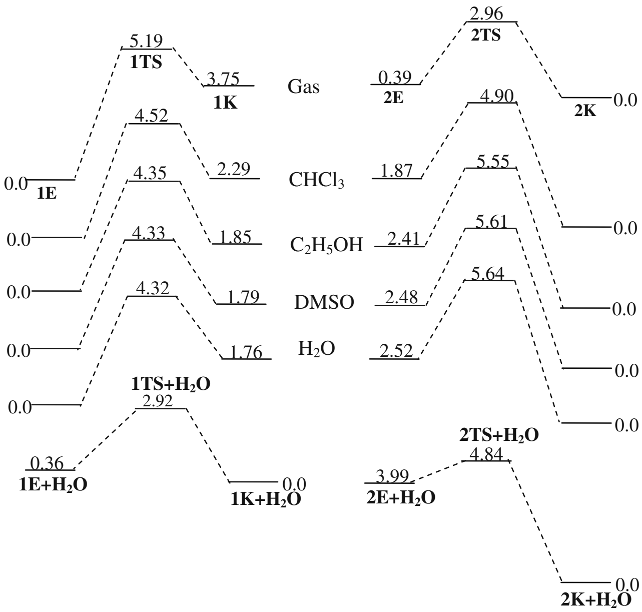

Fig. 3 Energy diagram in various solvents (IPCM) model and in the gas phase for isolated tautomers and water complexes

process of **1** and **2**, as it is seen in Fig. 3 the barrier to E → K process decreases with the increases of solvent polarity.

The energy difference between **2E** and **2K** tautomers is very small (0.39 kcal/mol) in the gas phase. The difference increases in the polar environment, i.e., **2K** form is 2.52 kcal/mol more stable than the **2E** in H_2O. The effect of solvation was greater on the **2K** tautomer than on the **2E** tautomer. Samely, the effect of solvation was greater on the **1K** tautomer than on the **1E**. The values of dipole moments, reported in the Table 2, are responsible for the larger stabilization of these forms (**1K** and **2K**) with respect to the gas phase calculations. The introduction of a solvent dielectric constant induces an increase in the dipole of the molecule, which occurs in a greater extent on the keto tautomers. As the solvent dielectric increases, a linear increase in the dipole is observed for each tautomer, since each of the keto forms has a higher dipol moment than the enol forms. Clearly, the keto forms have a greater solvation stabilization energy than the corresponding enol forms. While the energy difference of **2K** and **2E** tautomers was increased by 2.13 kcal/mol, the energy difference of 1E and 1K tautomers was decreased by 1.99 kcal/mol from gas phase to the most polar solvent (Fig. 4, Table 2). It is clear that an increase in the dielectric constants increases the stability of **1TS**, but decreases the stability of **2TS**. The heights of the calculated barriers of the 2E → 2K process slightly increase with increasing solvent polarity.

M.Asiri and co-workers [74] studied tautomerism in compounds **1** and **2** by using, IR, ^{1}H-NMR and UV-visible spectroscopy. The results have suggested that the anils prepared from 2-amino substituted pyridine exist mainly in enol form. On the other hand, compound 2 exists as a mixture of enol and keto form. Thus, this and other [59] experimental data is in very good agreement with our gas phase and IPCM calculations for these compounds. In order to gauge the possible importance of some specific solvent effects like H-bonds, calculations with the inclusion of one water molecule as solvent (see Fig. 5), to the enol-, keto-forms and TS structures have been carried out. We have performed calculations at the same level of theory for the complexes. The values of calculated uncorrected interaction energies, E_{int} and corrected interaction energies, $E_{int,cp}$ are given in the Table 3. The interaction energies were corrected for basisset superposition error (BSSE) at the B3LYP level using an approximation to the Boys- Bernardi counterpoise method [75] as per the details given below:

$$E_{int} = E(A)^m + E(B)^m - E(AB)$$
$$BSSE = E(A)^m - E(A)^c + E(B)^m - E(B)^c$$
$$E_{int,cp} = E_{int} - BSSE.$$

Where E(X) (X= A, B, AB) is the energy of molecules A, B or the complex AB. The superscript c or m refers either to the complex centered (c) or single molecule (m) basis set that is used to calculate the energy. It should be kept in mind that the geometry of A or B obtained in the optimized bimolecular system is not optimal for the isolated monomer and it exhibits a higher energy arrangement. So the energies of A and B were calculated at the optimized geometries of isolated molecules, keeping the ghost basis of the corresponding other molecule at the optimized geometry of the complex. Thus the calculation depends on the geometry of the complex.

Suprisingly, the complex **1K+H$_2$O** was found to be 0.36 kcal/mol more stable than the **1E+H$_2$O** complex. The calculated O....N distance (2.548 Å) in 1E indicates a medium strong H-bond. For **1K**, this distance is 2.617 Å.

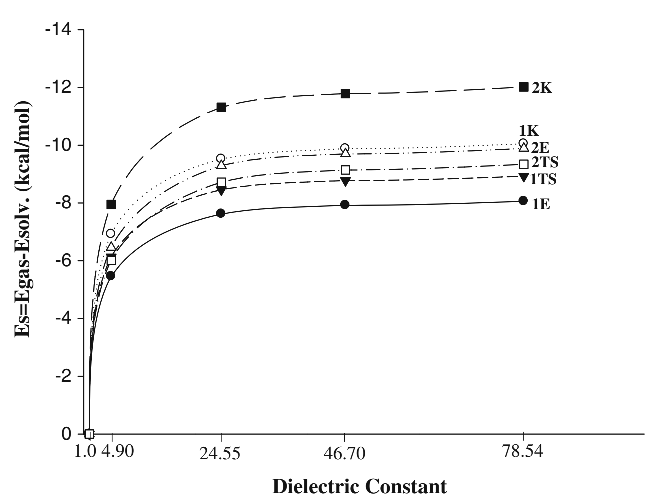

Fig. 4 Solvation energies (ΔEs) in kcal/mol for tautomers and TSs

Table 2 Dipol moments (in debye) and solvation energy ΔEs=Egas-Esolv. (kcal/mol) of both tautomeric forms in the gas phase and different solvents

	Gas phase	$CHCl_3$		C_2H_5OH		DMSO		H_2O	
	μ	ΔEs	μ	ΔEs	μ	ΔEs	μ	ΔEs	μ
1E	1.81	−5.46	2.46	−7.62	2.73	−7.92	2.76	−8.06	2.78
1K	3.28	−6.92	4.30	−9.52	4.68	−9.88	4.74	−10.05	4.76
1TS	2.71	−6.13	3.27	−8.46	3.49	−8.78	3.52	−8.93	3.53
2E	1.26	−6.46	1.70	−9.29	1.97	−9.70	2.01	−9.89	2.02
2K	2.48	−7.95	3.23	−11.31	3.65	−11.79	3.71	−12.02	3.74
2TS	1.74	−6.01	1.92	−8.72	1.92	−9.14	1.94	−9.34	1.96

As is seen from the data in Fig. 5, the complex **1K+H$_2$O** is lower in energy because it has a stronger hydrogen bond and a higher interaction energy. The complex **2E+H$_2$O** was found in calculation as 3.99 kcal/mol higher in energy than **2K+H$_2$O**. Considering the interaction distance water and Schiff base monomer, for the Schiff base **1**, in the keto-enamine form H_1....OH_2 (R=2.547 Å) and O_1...H_2O (R= 1.88 Å) preferable while in the enol-imine form H_1....OH_2 (R=2.670 Å) and O_1...H_2O (R=2.137 Å) interaction stabilizes more the anil-solvent system. Seemingly, the H_1....OH_2 and O_1....H_2O distances in **2K** are nearly 0.222 Å and 0.175 Å, respectively, shorter than the same distance in **2E**. It has been found that the keto-enamine form is more stable. ΔE_s in the IPCM field shows that the interaction between solvent and Schiff base monomer is the most stabilizing for the keto-enamine form in water and other polar solvent, which again is in very good agreement with the experimental results. The values of imaginary frequencies associated with the transition states of the monomer and complex were calculated as $-1074.25\ cm^{-1}$ and

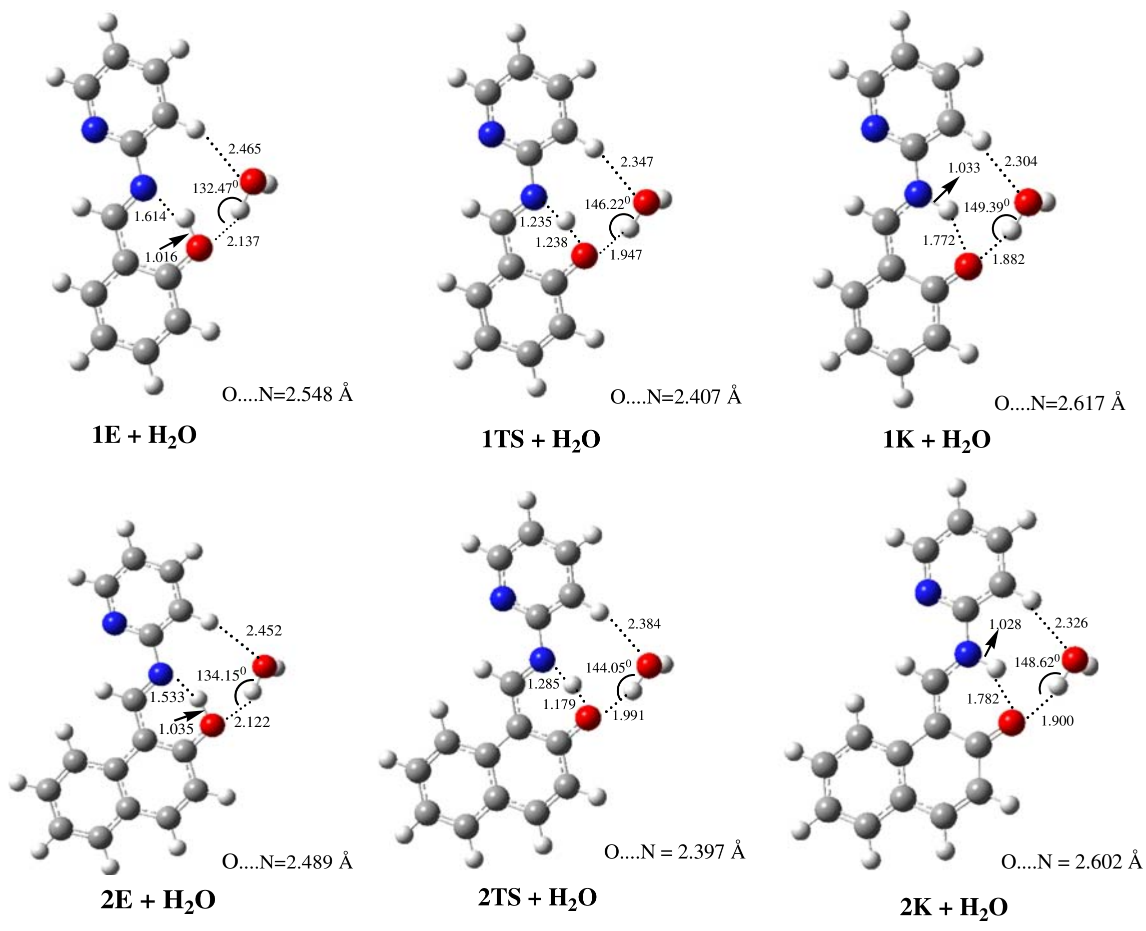

Fig. 5 Geometry-optimized structures of complexes and related transition states of the proton transfer process

Table 3 Interaction energies (in kcal/mol) of complexes

Structure	E_{int}	BSSE	$E_{int,cp}$
1E + H_2O	7.44	3.62	3.82
1TS + H_2O	10.13	4.10	6.21
1K + H_2O	11.55	3.92	7.63
2E + H_2O	7.37	3.62	3.75
2TS + H_2O	9.10	3.95	5.15
2K + H_2O	10.98	3.94	7.04

−1109.50 cm^{-1} for molecule **1** and to be −1154.80 cm^{-1} and −998.98 cm^{-1} for molecule **2**, respectively. For the 1E 1K process, the barrier of the monomer is 5.19 kcal/mol in the gas phase and 4.32 kcal/mol in the water solutions, the barrier decreases to 1.56 kcal/mol and, when the Schiff base **1** complexes with one water molecule. For the 2E 2K process the barrier in the gas phase and in the solution was calculated as 4.90 and 3.12 kcal/mol for the monomer, and 0.85 kcal/mol for the complexes. Therefore, the tautomerization mediated by hydrogen bonding to a water molecule, so the so-called “solvent assisted proton transfer reaction” [76, 77] significantly lower the reaction barrier. Moreover, the barrier of **1+H₂O** complex is higher than those of the **2+H₂O** complex. Probably, due to stronger hydrogen bonding interaction on of the **2+H₂O** complex. Strengthening of the distance $O_1H...N$ and weakening of the distance $NH...O_1$ by polar solvents concomitant shift of the tautomeric equilibrium toward the keto-enamine form.

Transition structures correspond with a intramolecular hydrogen transfer between N_1 and O_1 atoms. The large

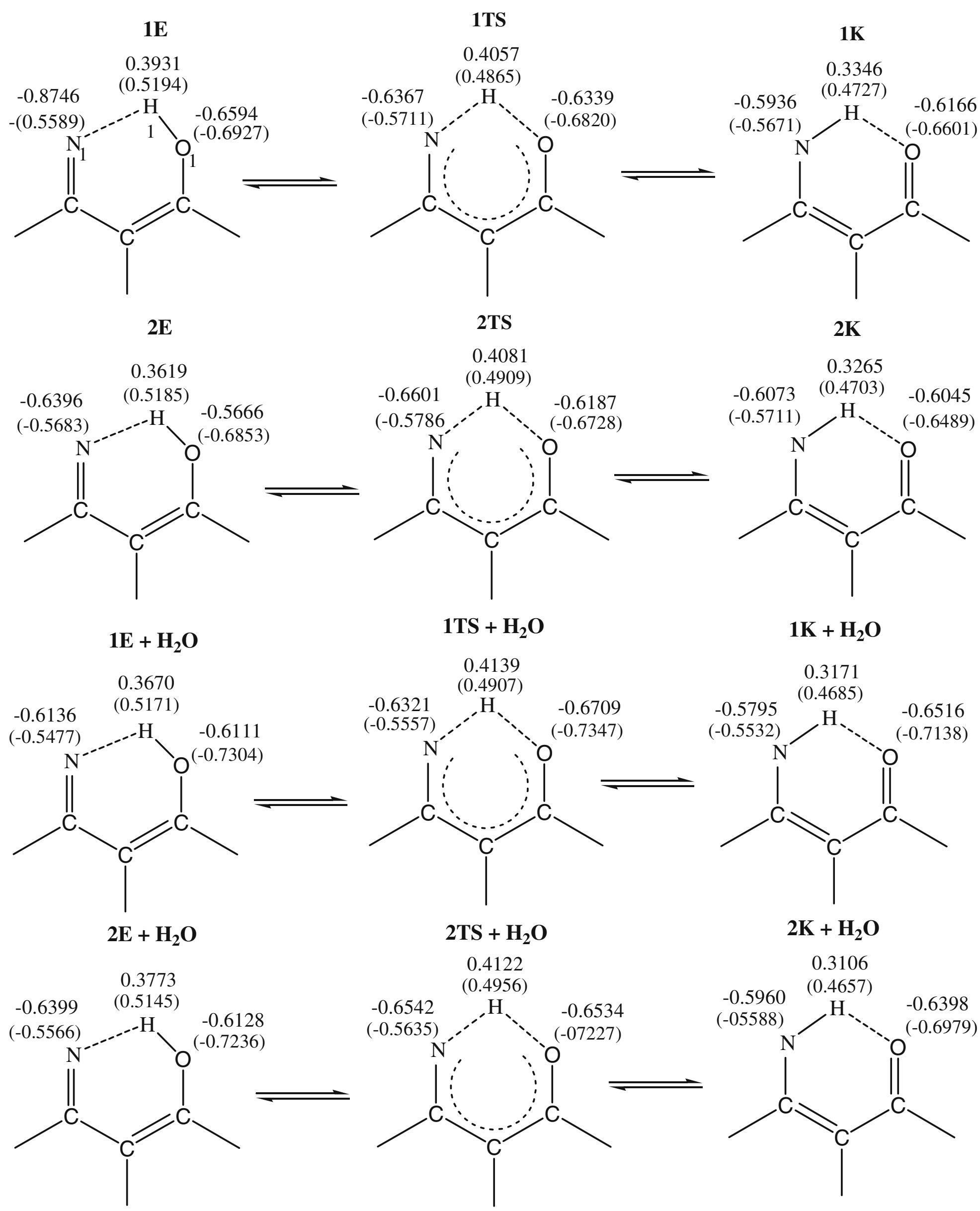

Fig. 6 Selected NBO and Mulliken (in parenthesis) charge populations of isolated and monohydrated tautomers

value of the relative energies of these TSs in the gas phase prevents the transformation between the different tautomers. It is important to remark that larger value of barrier heights can be diminished by the inclusion of the discrete water molecules acting as the bifunctional catalyst. Therefore, the separete tautomers may not interconvert readily, but they probably do very rapidly in real water.

Charges

NBO charge distribution was also analyzed according to the results calculated at the B3LYP/6-31G** level. The selected NBO and Mulliken charge distribution is shown in Fig. 6. For analyzing these results, it would be useful to follow the evolution of charge separation along the reaction path. We have considered the charge on labile hydrogen H_1, O_1 and N_1 and so on. The Mulliken and NBO charge populations show that there is a high positive charge on the hydrogen atom during the process in all cases, which could suggest that the reaction corresponds to a proton transfer. And the proton transfer proceeds through a three-center interaction. As we all know, the net charge of donor oxygen is expected to increase in a typical proton transfer process, whereas that of the acceptor nitrogen is expected to decrease. It can be seen from Fig. 6 that the net charges of donor oxygen decreases, on the contrary, the charge of acceptor nitrogen increases during the E → K process. The population of charge for the donor oxygen is much larger than that of the acceptor nitrogen. So, there is a π-electronic transfer from the donor oxygen to the acceptor nitrogen through the conjugated π-system. In addition, the charge population of active hydrogen and acceptor nitrogen in a **2E** form is larger than that in the **1E** form. So, the hydrogen transfers in compound **2** more easiliy than that in compound **1**, and the interaction between active hydrogen and acceptor nitrogen (E → K) will be propitious to the dissociation of hydrogen, that is, its acidic character increases in the enol-imine form. The charge on labile hydrogen H_1 decreases during the process of intramolecular proton transfer and its positive charge becomes more positive in the enol-imine forms.

Conclusions

The molecular structures and intramolecular proton transfer reaction for the title compounds are theoretically investigated with ab initio method as well as the density functional theory. The results showed that the keto-enamine from **2E** is dominant in both the gas phase and all dielectric media. The energy barrier of proton transfer is predicted to be 2,57 kcal/mol for the 2E → 2K tautomerization in the gas phase. However, in the polar medium, these barrier decreases to 0.85 kcal/mol through a solvent assisted proton transfer process mediated by a specific water molecule and tautomeric equilibrium in which the keto-enamine form dominates is quickly reached.

In the case of Schiff base monomer **1**, the enol-imine form is more stable in the gas phase and keto-enamine form is considerably stabilized by increasing solvent polarity and favored with the inclusion of one water molecule. The height of the barriers of tautomerization 1E → 1K considerable decrease with increasing solvent polarity.

Acknowledgements We thank Cumhuriyet University, Sivas (Turkey) for access to the Gaussian 03 program packages

References

1. Inabe T (1991) New J Chem 15:129–136
2. Feringa BL, Jager WF, De Lange B (1993) Tetrahedron 49:8267–8310
3. Todd MD, Todd RH, Mikkelsen KV (1994) J Mol Struct 120:49–71
4. Lewis JW, Sandorfy C (1982) Can J Chem 60:1727–1737
5. Becker RS, Lenoble C, Zein A (1987) J Phys Chem 91:3509–3517
6. Inabe T, Luneau I, Mitani T, Maruyama Y, Takeda S (1994) Bull Chem Soc Jpn 67:612–621
7. Seliger J, Zagar V, Blinc R, Hadjoudis E, Milia F (1990) Chem Phys 142:237–244
8. Ledbetter JW Jr (1968) J Phys Chem 72:4111
9. Alarcón SH, Olivieri AC, Labadie GR, Cravero RM, González-Sierra M (1995) Tetrahedron 51:4619–4626
10. Alarcón SH, Olivieri AC, Labadie GR, Cravero RM, Labadie G, González-Sierra M (1995) J Phys Org Chem 8:713–720
11. Alarcón SH, Olivieri AC, Nordon A, Haris RK (1996) J Chem Soc Perkin Trans 2:2293–2296
12. Yildiz M, Kilic Z, Hokelek T (1998) J Mol Struct 441:1–10
13. Kessissoglou DP, Raptopoulou CP, Bakalbassis EG, Terzis A, Mrozinski J (1992) Inorg Chem 31:4339–4345
14. Bhatia SC, Bindlish JM, Saini AR, Jain PC (1981) J Chem Soc Dalton Trans.1773–1779
15. Calligaris M, Nardin G, Randaccio L (1972) Coord Chem Rev 7:385–403
16. Maslen HS, Waters TN (1975) Coord Chem Rev 17:137–176
17. Stewart J, Lingafelter EC (1959) Acta Crystallogr 12:842–845
18. Chen D, Martel AE (1987) Inorg Chem 26:1026–1030
19. Pyrz JW, Roe AL, Stern LJ, Que L Jr (1985) J Am Chem Soc 107:614–620
20. Costamagna J, Vargas J, Latorre R, Alvarado A, Mena G (1992) Coord Chem Rev 119:67–88
21. Dixon NE, Gazzalo C, Watters JJ, Blakeley RL, Zerner B (1975) J Am Chem Soc 97:4131–4133
22. Walsh CT, Orme-Johnson WH (1987) Biochemistry 26:4901–4906
23. Nagy P, Harzfeld R (1998) Spectr Lett 31:221–232
24. Kamounah FS, Salman SR, Mahmoud AAK (1998) Spect Lett 31:1557–1567
25. Rospenk M, Król-Starzomska I, Filarowski A, Koll A (2003) Chem Phys 287:113–124
26. Cohen MD, Flavian S, Leiserowitz L (1967) J. Chem. Soc. B 329–334

27. Harzfeld R, Nagy P (2001) Curr Org Chem 5:373–394
28. Dudek GO, Dudek EP (1966) J Am Chem Soc 88:2407–2412
29. Dziembowska T, Rozwadowski Z, Filarowski A, Hansen PE (2001) Magn Reson Chem 39:67–87
30. Salman SR, Saleh NAI (1997) Spectr Lett 30:1289–1300
31. Kownacki K, Mordzinski A, Wilbrandt R, Grabowska A (1994) Chem Phys Lett 227:270–276
32. Grabowska A, Kownacki K, Kaczmarek L (1994) J Lumin. 60-1:886–890
33. Ogawa K, Harada J, Fujiwara T, Yoshida S (2001) J Phys Chem A 105:3425–3427
34. Ledbetter JW Jr (1977) J Phys Chem 81:54–59
35. Cohen MD, Flavian S (1967) J Chem Soc. B 317
36. Allen M, Roberts JD (1980) J Org Chem 45:130–135
37. Percy GC, Thornton DA (1972) J Inorg Nucl Chem 34:3357–3367
38. Salman SR, Lindon JC, Farrant RD, Carpenter TA (1993) Magn Reson Chem 31:991–994
39. Gavranic M, Kaitner B, Mestrovis E (1996) J Chem Crystallogr 26:23–28
40. Kaitner B, Pavlovic G (1996) Acta Crystallogr C 52:2573–2575
41. Zgierski M, Grabowska A (2000) J Chem Phys 113:7845–7852
42. Kletski M, Milov A, Metelisa A, Knyazhansky M (1997) J Photochem Photobiol A 110:267–270
43. Fernández-G JM, del Rio-Portilla F, Quiroz-García B, Toscano RA, Salcedo R (2001) J Mol Struct 561:197–207
44. Antonov L, Fabian MF, Nedeltcheva D, Kamounah FS (2000) J Chem Soc Perkin Trans 2:1173–1179
45. Joshi H, Kamounah FS, van der Zwan G, Gooijer C, Antonov L (2001) J Chem Soc Perkin Trans 12:2303–2308
46. Herzfeld R, Nagy P (1999) Spectrosc Lett 32:57–71
47. Unver H, Zengin DM, Guven K (2000) J Chem Crystallogr 30:359–364
48. Popović Z, Roje V, Pavlović G, Matković-Čalogović D, Giester G (2001) J Mol Struct 597:39–47
49. Hadjoudis E, Vitterakis M, Maustakali-Marridis I (1987) Tetrahedron 43:1345–1360
50. Hamilton DE, Drago RS, Zombeck A (1987) J Am Chem Soc 109:374–379
51. Nishida Y, Kino K, Kida S (1987) J Chem Soc Dalton Trans 1157–1161
52. Becke AD (1993) J Chem Phys 98:5648–5652
53. Becke AD (1993) J Chem Phys 98:1372–1377
54. Lee C, Yang W, Parr RG (1988) Phys Rev B 37:785–789
55. Foresman JB, Keith TA, Wiberg KB, Snoonian J, Frisch MJ (1996) J Phys Chem 100:16098–16104
56. Reed AE, Curtiss LA, Weinhold F (1988) Chem Rev 88:899–926
57. Reed AE, Weinstock RB, Weinhold F (1985) J Chem Phys 83:735–746
58. Frisch MJ et al (2003) Gaussian, Inc., Pittsburgh PA
59. Nazir H, Yildiz M, Yilmaz H, Tahir MN, Ulku D (2000) J Mol Struct 524:241–250
60. Moustakali-Mavridis I, Hadjoudis E, Mavridis A (1978) Acta Crystallogr Sect B 34:3709–3715
61. Gilli P, Bertolasi V, Ferretti V, Gilli G (2000) J Am Chem Soc 122:10405–10417
62. Gavranic M, Kaitner B, Mestrovic E (1996) J Chem Crystallogr 26:23–28
63. Allen FH, Kennard O, Watson DG, Brammer L, Orpen AG, Taylor R (1987) J Chem Soc Perkin Trans 2:S1–S19
64. Kaitner B, Pavlovic G (1996) Acta Crystallogr Sect C 52:2573–2575
65. Elmali A, Kabak M, Kavlakoglu E, Elerman Y, Durlu TN (1999) J Mol Struct 510:207–214
66. Hokelek T, Gunduz N, Hayvali Z, Kilic Z (1995) Acta Crystallogr C 51:880–884
67. Hokelek T, Gunduz N, Hayvali Z, Kilic Z (1995) J Chem Crystallogr 25:831–836
68. Elerman Y, Svoboda I, Fuess ZH (1991) Kristallogr 196:309–311
69. Elerman Y, Elmali A, Kabak M, Aydin M, Peder M (1994) J Chem Cryst 24:603–606
70. Elerman Y, Elmali A, Svoboda I (1995) Acta Cryst C 51:2344–2346
71. Elmali A, Ozbey S, Kendi E, Kabak M, Elerman Y (1995) Acta Cryst C 51:1878–1880
72. Ledesma G, Ibanez G, Escandar G, Olivieri AC (1997) J Mol Struct 415:115–121
73. Salman SR, Shawkat SH, Al-Obaidi GM (1990) Can J Spectrosc 35:25–27
74. Asiri MA, Badahdah KO (2007) Molecules 12:1796–1804
75. Boys SF, Bernardi F (1970) Mol Phys 19:553–&
76. Rodriquez CF, Cunje A, Shoeib T, Chu IK, Hopkinson AC, Siu KWM (2000) J Phys Chem A 104:5023–5028
77. Liang JY, Lipscomb WN (1987) Biochemistry 26:5293–5301